Electron-electron collision dynamics of the four-electron escape in Be close to threshold

A. Emmanouilidou[1,2] and H. Price[1]

[1]*Department of Physics and Astronomy, University College London, Gower Street, London WC1E 6BT, United Kingdom*

[2]*Chemistry Department, University of Massachusetts at Amherst, Amherst, Massachusetts, 01003, USA*

(Received 20 November 2012; published 29 April 2013)

We explore the escape geometry of four electrons a few eV above threshold following single-photon absorption from the ground state of Be. We find that the four electrons leave the atom on the vertices of a triangular *pyramid* instead of a previously predicted regular tetrahedron. To illustrate the physical mechanisms of quadruple ionization we use a *momentum transferring attosecond collision* scheme which we show to be in accord with the triangular pyramid breakup pattern.

DOI: 10.1103/PhysRevA.87.043428 PACS number(s): 32.80.Fb

Exploring the correlated electronic motion during ionization of multielectron atoms and molecules, for energies close to the ionization threshold, is a fundamental and challenging task in physics. This electronic correlation has been a topic of intense interest (for recent work see Refs. [1,2]) since Wannier's pioneering work [3]. According to Wannier's law $\sigma \propto E^{\beta}$ for excess energies $E \to 0$, where σ is the cross section of the process involved and β depends on the number and type of particles involved in the breakup process. Using classical mechanics, Wannier also showed that two electrons moving in the Coulomb field of an ion escape back-to-back for energies $E \to 0$. Extending Wannier's work, later studies predicted a three-electron breakup on the vertices of an equilateral triangle [4,5] and a four-electron breakup on the vertices of a regular tetrahedron [5,6]. While these highest-symmetry breakup patterns were predicted for $E \to 0$, it is generally expected that they also prevail for excess energies a few eV above threshold where the threshold Wannier exponent β is still retrieved. In this work we show that this is not true.

We show that for single-photon quadruple ionization (QI) from the ground state of Be the prevailing breakup pattern a few eV above threshold is different than the one predicted for $E \to 0$. For single-photon triple ionization from the ground state of Li we have already shown that the breakup pattern is not the expected "triangle" but a T shape a few eV above threshold [7]. In the T shape two electrons escape back-to-back while the third electron escapes at 90° with respect to the other two electrons. Very recently, further evidence for the T shape was provided by fully quantum mechanical calculations for energies 5 eV above the triple ionization threshold of the ground state of Li [8]. The previously predicted triangle pattern was, however, observed in recent $(e,3e)$ coincidence measurements for electron impact on the ground state of He [9]. The above reinforce a prediction we made in Ref. [10] that the three-electron breakup pattern depends on the initial state and can be either a T shape or a triangle.

In the current work, we present evidence that for single-photon QI from the ground state of Be, a few eV above threshold, the prevailing breakup pattern is a triangular *pyramid*. That is, the three electrons escape on the vertices of an equilateral triangle at 120° from each other and the other electron escapes perpendicular to the plane of the three electrons. Our prediction differs from the symmetric four-electron escape on the vertices of a regular tetrahedron predicted in the limit $E \to 0$ [5,6]. However, for four-electron escape we find that two more breakup patterns of higher symmetry, a regular tetrahedron and a square, previously predicted in Ref. [5], are also present. Thus, the deviation from the Wannier breakup patterns is larger for three electrons. This suggests the possibility that as the number of electrons increases the prevailing breakup patterns are more consistent with those predicted by Wannier. Moreover, uncovering the physical mechanisms of QI, we express the multielectron escape dynamics in terms of *momentum transferring attosecond collision sequences*. Thus, besides addressing a fundamental law of physics, we also elucidate correlated electronic motion in multielectron escape. This is of high interest since the advent of ultrashort and intense laser pulses has brought time-resolving correlated electron dynamics in intra-atomic ionization processes to the forefront of attosecond science [11–15].

Given computational capabilities, addressing four-electron escape with quantum mechanical techniques is currently out of reach [16]. Classical mechanics is justified for excess energies close to threshold as detailed in the original work of Wannier [3] and in subsequent work on two-electron [17] and three-electron atoms. Specifically, for three-electron escape by single-photon absorption in Li, using the quasiclassical technique we use in the current work, we computed the total differential cross section in Ref. [7] which is in very good agreement with the experimental results in Ref. [18]. We also found the Wannier exponent in Ref. [19] equal to 2.15 in very good agreement with the theoretical value of 2.16 [4] and we computed the differential cross sections in energy [20] which agree very well with the quantum results in Ref. [21]. We tackle quadruple photoionization using the quasiclassical technique—quasi due to the choice of initial state—detailed in Ref. [22]. Briefly, using the classical trajectory Monte Carlo method [23,24], we propagate in time the full five-body Hamiltonian accounting for all interactions to all orders. In addition, we use a Wigner [25] distribution for setting up the initial phase space of the bound electrons [26]. We note that the quasiclassical technique we use for QI has produced a number of results for three-electron atoms in very good agreement with either experimental or quantum mechanical results. We compute the probability for QI, P^{4+}, for excess energies ranging from 3 to 10 eV. 3 eV is close to threshold

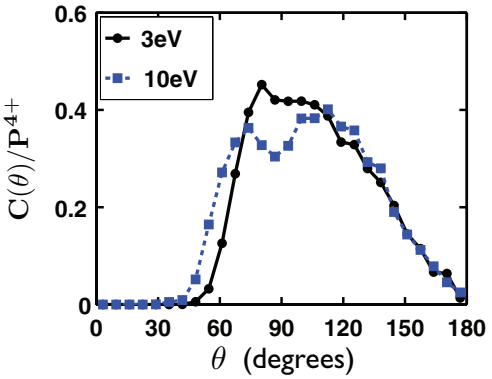

FIG. 1. (Color online) Probability for two electrons to escape with an interelectronic angle θ for excess energies of 3 eV (black dots with solid line) and 10 eV (blue squares with dashed line). To guide the eye, for each excess energy, we connect the symbols representing our data with a line.

(399 eV) and the computational time involved is not prohibitive for obtaining good statistics. 10 eV is an upper bound estimate of excess energies where the Wannier exponent β can still be retrieved. Using our data for P^{4+} from 3 to 10 eV in steps of 1 eV we find β equal to 94% of the theoretically predicted value of 3.288 [5]. In the framework of Wannier's theory, in what follows we discuss our results for 3 and 10 eV.

To identify the four-electron escape pattern we focus on an observable that naturally encompasses electronic correlation. Such an observable is the probability for two electrons to escape with an interelectronic angle θ—we refer to it as angular correlation probability $C(\theta)$. In Fig. 1, we plot $C(\theta)$ for 3 and 10 eV excess energies. Given that P^{4+} is 1.8×10^{-10} for 3 eV and 7.3×10^{-9} for 10 eV the computational task involved is immense. Nevertheless, to provide good accuracy, for each excess energy we consider, our results involve roughly 10^4 quadruple ionization events. In Fig. 1, we see that for 10 eV $C(\theta)$ has two peaks: one around 74° and a second one around 100°–125°. However, for 3 eV it is not clear whether only one or two less pronounced peaks—compared to 10 eV—are present in the range 80°–112°. In Fig. 1, $C(\theta)$ is plotted using 28 bins for θ. We choose the bin size so that the double-peak structure in $C(\theta)$ is best resolved given the limitations imposed by our statistics.

To what four-electron escape geometry does the shape of $C(\theta)$ correspond to? A regular tetrahedron pattern with all electrons escaping at 109.5° from each other would result in a single peak in $C(\theta)$. A square pattern with two interelectronic angles being 180° and four interelectronic angles being 90° would result in two peaks in $C(\theta)$ with the peak at 90° twice as high as the peak at 180°. A triangular *pyramid* pattern with three electrons escaping at 120° from each other and the other electron escaping at 90° from the three electrons would result in two peaks in $C(\theta)$ of equal height. Hence, the double peak in $C(\theta)$ (Fig. 1) for 10 eV is consistent with a triangular pyramid shape. For 3 eV the shape of $C(\theta)$ does not provide conclusive evidence for the prevailing escape geometry.

We next elucidate the physical mechanisms of QI and provide conclusive evidence for the breakup patterns the four electrons follow. How does the photoelectron redistribute the energy it gains from the photon to the remaining three electrons? This is a natural question in the framework of classical mechanics where the electrons undergo soft collisions mediated by Coulomb forces. To answer this question, we use a classification scheme similar to the one we first introduced in the context of three-electron escape following single-photon absorption from the ground state of Li [7]. That is, we define a collision between electrons i and j—labeling it as $\widehat{ij}$—through the momentum transfer

$$\mathbf{D}_{ij} = \int_{t_1}^{t_2} \nabla V(r_{ij}) dt \tag{1}$$

under the condition that $V(r_{ij}(t_k))$ are local minima in time with $t_2 > t_1$ while $r_{ij} = |\mathbf{r_i} - \mathbf{r_j}|$ and $V(r_{ij}) = 1/|\mathbf{r_i} - \mathbf{r_j}|$. During the time interval $t_1 < t < t_2$ all five particles interact with each other. Hence, the above definition is meaningful if the collision redistributes energy primarily within the three-body subsystem that includes the nucleus and the electrons i and j. For automated identification of the collisions, we need sensitivity thresholds to register only the important collisions for the quadruple events. Due to the significantly higher complexity of the four-electron problem we introduce two sensitivity thresholds instead of one for three electrons [7,27]. We do so for each individual QI trajectory by forming the maximum $D = \max_{i \neq j} |\mathbf{D}_{ij}|$ and registering only collisions with $|\mathbf{D}_{ij}|/D > \delta$, where $i, j = 1,2,3,4$. We introduce another sensitivity threshold for how "sharp" a collision is. Namely, if electron i gains energy through more than one collision, we find the maximum $\Delta V_i = \max_{i \neq j}[V(r_{ij})^{\max} - V(r_{ij})^{\min}]$, with $V(r_{ij})^{\max/\min}$ being the max or min value of $V(r_{ij}(t))$ for $t_1 < t < t_2$, and register only collisions satisfying $[V(r_{ij})^{\max} - V(r_{ij})^{\min}]/\Delta V_i > \delta_1$. We have checked that our results and conclusions do not change for different values of δ and δ_1; we choose $\delta = 1/12$ and $\delta_1 = 1/8$.

According to this classification scheme we find that electrons 2, 3, and 4 gain sufficient energy to leave the atom through two prevailing ionization routes. We denote by electron 1 the photoelectron (from a 1s orbital), by 2 the other 1s electron, and by 3 and 4 the two 2s electrons. In the first route the photoelectron 1 knocks out first electron 2 and then proceeds to knock out electrons 3 and 4. That is, first a collision $\widehat{12}$ takes place very early in time and roughly 24 as later collisions $\widehat{13}$ and $\widehat{14}$ occur. With collisions $\widehat{13}$ and $\widehat{14}$ taking place close in time we find that a fourth collision, $\widehat{34}$, can occur in addition to the previous three collisions. We refer to this ionization route where the photoelectron transfers energy to both electrons 3 and 4 as $s_1 = \{\widehat{12},\widehat{13},\widehat{14}\}$. In the second route, the photoelectron 1 first knocks out electron 2 through the collision $\widehat{12}$. Then, electron 2 becomes the new impacting electron knocking out, roughly 24 as later, electrons 3 and 4 through the collisions $\widehat{23}$ and $\widehat{24}$. With collisions $\widehat{23}$ and $\widehat{24}$ taking place close in time a fourth collision, $\widehat{34}$, can occur in addition to the previous three collisions. We refer to this ionization route where electron 2 transfers energy to both electrons 3 and 4 as $s_2 = \{\widehat{12},\widehat{23},\widehat{24}\}$. s_1 accounts for 41%, both for 3 eV and 10 eV, and s_2 for 24% for 3 eV and 26% for 10 eV of all QI events. Using this scheme of momentum transferring attosecond collision sequences we have

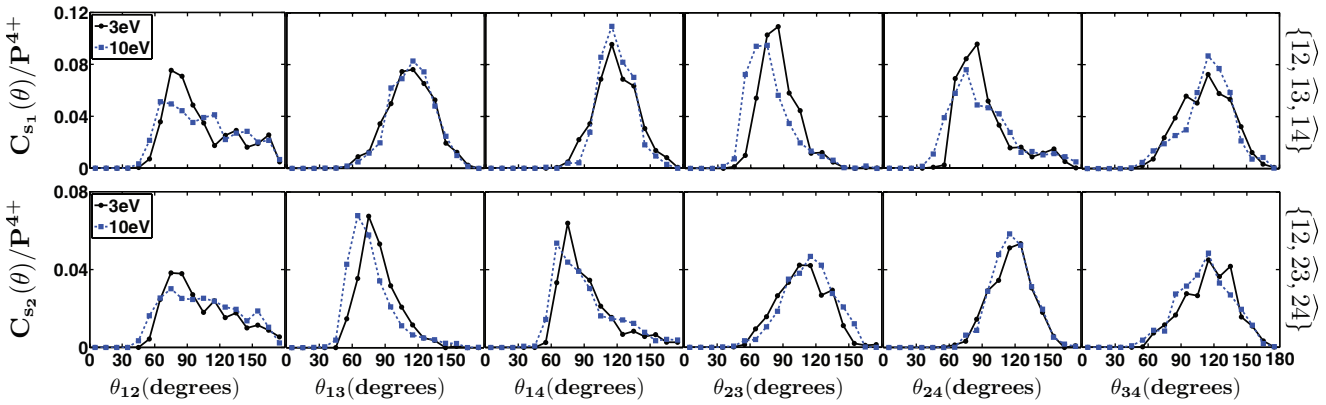

FIG. 2. (Color online) Same as Fig. 1 but for each interelectronic pair θ_{ij} for the ionization routes s_1 (top row) and s_2 (bottom row).

thus obtained a physical picture of the correlated electronic motion in an intra-atomic ionization process. Further, this scheme offers insight in choosing the appropriate asymptotic observables for inferring the temporal profile of electron-electron collision dynamics [28]. This is important since developing pump-probe schemes to time-resolve correlated multielectron escape is one of the current challenges facing attoscience [29].

In what direction do the four electrons escape in pathways s_1 and s_2? For s_1, at the time when all electrons to be ionized have received enough energy to leave the atom, the spatial electron distribution, we refer to it as transient threshold configuration (TTC) [10], is $r_1 \approx r_3 \approx r_4 \neq r_2$. That is, the last colliding electrons 1, 3, and 4 have $r_1 \approx r_3 \approx r_4$, which is close to the fixed point (see below) of the four-body Coulomb problem—three electrons and the nucleus. Thus, one expects that electrons 1, 3, and 4 will escape symmetrically on a plane at 120° from each other. In Fig. 2 (top row) we plot $C(\theta)$ for each of the six interelectronic angles of escape using only the QI events that correspond to the s_1 pathway; i.e, we plot $C_{s_1}(\theta)$. Indeed, we see that $C_{s_1}(\theta)$ for θ_{13}, θ_{14}, and θ_{34} peaks around 115°, for both 3 and 10 eV, corresponding to electrons 1, 3, and 4 escaping on the vertices of a triangle. (We note that the distributions in Figs. 1 and 2 are convoluted by the polar angle volume element $\sin\theta$ resulting in a peak at 120° being shifted to slightly smaller angles while a peak at 90° is not affected). In addition, we see that $C_{s_1}(\theta)$ for θ_{12}, θ_{23}, and θ_{24} peaks around 65°–75° and 75°–85° for 10 and 3 eV, respectively. Note that the shifting of the peak at smaller angles from 65°–75° for 10 eV to 75°–85° for 3 eV shows a tendency towards the triangular-pyramid-consistent angle of 90°. Thus, the distributions in Fig. 2 (top row) for the s_1 ionization route are consistent with the triangular pyramid shape shown in Fig. 3(a). Similarly for the ionization route s_2, $C_{s_2}(\theta)$ for θ_{23}, θ_{24}, and θ_{34} peaks around 115° while $C_{s_2}(\theta)$ for θ_{12}, θ_{13} and θ_{14} peaks around 65°–75° and 85° for 10 and 3 eV, respectively (Fig. 2 bottom row). These distributions are consistent with the triangular pyramid shape shown in Fig. 3(b). Therefore, for the majority (65%) of QI events the four electrons escape on the vertices of a triangular pyramid.

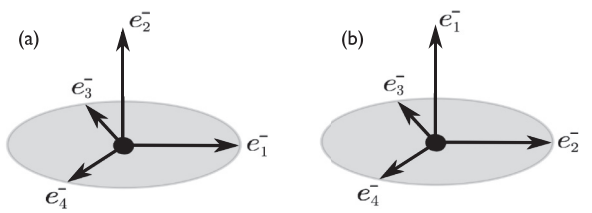

FIG. 3. The triangular pyramid escape geometry for four electrons corresponding to collision sequences s_1 (a) and s_2 (b).

We now provide further evidence that if the three electrons escape on a plane at 120° from each other then the preferred escape geometry of the other electron is perpendicular to this plane. We do so analytically by expressing the five-body Hamiltonian in hyperspherical coordinates:

$$H = \frac{p_r^2}{2} + \frac{\Lambda^2}{2R^2} + \frac{C(\mathbf{\Omega})}{R}, \tag{2}$$

where $\mathbf{\Omega} = (\alpha_1,\alpha_2,\alpha_3,\theta_1,\theta_2,\theta_3,\theta_4,\chi_1,\chi_2,\chi_3,\chi_4)$ contains all angular variables describing the positions of the electrons and Λ is a function of $\mathbf{\Omega}$ and all conjugate momenta. The total Coulomb interaction $V = C/R$ acquires in this form simply an angular-dependent charge $C(\mathbf{\Omega})$. The hyperspherical coordinates are given by

$$\begin{aligned} R &= \sqrt{r_1^2 + r_2^2 + r_3^2 + r_4^2}, \quad \chi_1 = \phi_3 - \phi_1, \\ \alpha_1 &= \arctan\left(\frac{r_1}{r_3}\right), \quad \chi_2 = \phi_4 - \phi_1, \\ \alpha_2 &= \arctan\left(\frac{\sqrt{r_1^2 + r_3^2}}{r_4}\right), \quad \chi_3 = \phi_2 - \phi_1, \\ \alpha_3 &= \arctan\left(\frac{\sqrt{r_1^2 + r_3^2 + r_4^2}}{r_2}\right), \quad \chi_4 = \phi_1 + \phi_2 + \phi_3 + \phi_4, \end{aligned} \tag{3}$$

where ϕ_i and θ_i are the azimuthal and polar angles of the ith electron. Focusing on s_1, the TTC is $r_1 \approx r_3 \approx r_4 \neq r_2$. For simplicity we assume $r_1 \approx r_3 \approx r_4 \ll r_2$, resulting in $\alpha_3 \approx 0$ (the opposite case would lead to the same result). We then expand $C(\mathbf{\Omega})$ in powers of α_3:

$$C(\mathbf{\Omega}) \approx \alpha_3^{-1} \sum_{n=0}^{3} c_n \alpha_3^n. \tag{4}$$

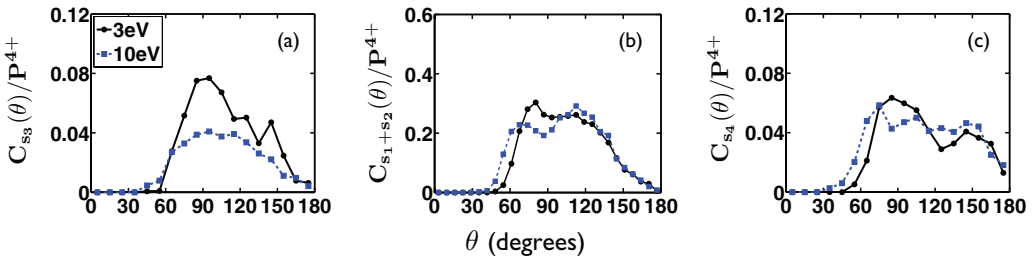

FIG. 4. (Color online) $C(\theta)$ for the ionization routes s_3 (a), $s_1 + s_2$ (b), and s_4 (c). The lower statistics in panels (a) and (c) compared to those in panel (b) dictate using 18 [(a) and (c)] instead of 28 (b) bins.

The lowest-order term in α_3 is the potential term of the four-body Coulomb problem with $Z = 4$. Thus, the problem of finding a stable configuration is that of the three-electron problem with the solution $\alpha_1^* = \pi/4$, $\alpha_2^* = \arctan(\sqrt{2})$, $\chi_1^* = 2\pi/3$, $\chi_2^* = 4\pi/3$, and $\theta_1 = \theta_3 = \theta_4 = 90^\circ$ [10]. These values minimize c_2 for any value θ_2. Minimizing c_3 with respect to θ_2 we find the stable solution $\theta_2 = 0^\circ$ which indeed corresponds to a triangular pyramid breakup geometry, which is of lower symmetry than a regular tetrahedron.

It is now clear that for the $s_1 + s_2$ labeled QI events the four electrons escape on the vertices of a triangular pyramid (see Fig. 2). Since these events account for roughly 65% of all QI events the triangular pyramid shape prevails for 3 and 10 eV excess energy. Why then is the double peak in $C(\theta)$ for 10 eV more pronounced than that for 3 eV in Fig. 1? One reason is the following: an analysis of $C_{s_1}(\theta)$ and $C_{s_2}(\theta)$ (Fig. 2) shows that for $C_{s_1+s_2}(\theta)$ [Fig. 4(b)] the two peaks are closer for 3 eV (at 85° and 115°) than for 10 eV (at 65°–75° and 115°), resulting in a stronger overlap and a less pronounced double peak for 3 eV. The same effect is also present when all QI events are considered in $C(\theta)$ in Fig. 1. Another reason is an ionization route which involves at least four distinct collisions: one collision is $\widehat{12}$ while two of them involve electrons 3 and/or 4 each gaining energy by both electrons 1 and 2—we label this route as s_3. For s_3 TTC is $r_1 \approx r_3 \approx r_4 \approx r_2$. This spatial distribution is close to the fixed point of the five-body Coulomb problem corresponding to all four electrons escaping on the vertices of a regular tetrahedron at 109.5° from each other. Indeed, in Fig. 4(a) we find that $C_{s_3}(\theta)$ has a single peak consistent with a regular tetrahedron geometry. As expected this single peak becomes sharper with decreasing excess energy; compare $C_{s_3}(\theta)$ for 10 and 3 eV in Fig. 4(a). Thus, when all ionization routes are considered the contribution of $C_{s_3}(\theta)$ for 10 eV does not smear out the double peak of $C_{s_1+s_2}(\theta)$ [see Fig. 4(b)], while it does so for 3 eV. Further contributing to the difference in the shape of $C(\theta)$ between 3 and 10 eV is that the percentage contribution of s_3 to all QI events increases with decreasing excess energy from 7% for 10 eV to 11% for 3 eV. Note that while the regular tetrahedron does not prevail in the breakup geometry, as generally expected, it is nevertheless present. The same is true for another high symmetry breakup pattern which results from yet another ionization route that involves mainly three distinct collisions. One collision is $\widehat{12}$ while the other two collisions involve electrons 3 and 4 each gaining energy by different electrons; i.e., if electron 3 gains energy from electron 1 then electron 4 gains energy from electron 2. This route which we label as s_4 accounts for roughly 10% of all QI events for 3 and 10 eV excess energies. We find that for 3 eV $C_{s_4}(\theta)$ in Fig. 4(c) has two peaks at 90° and 150° with the peak at 90° being almost twice as high as the peak at 150°. This is consistent with the four electrons escaping on the apexes of a square [30] with four interelectronic angles being 90° and two being 180° (the peak at 180° is shifted at 150° in Fig. 4(c) since the distribution is convoluted by $\sin\theta$). This planar breakup geometry was previously predicted in Ref. [5].

In conclusion, we have shown that a triangular pyramid is the prevailing breakup pattern for QI by single-photon absorption from the ground state of Be for excess energies as low as 3 eV above threshold. This pattern can be verified by future quantum mechanical and experimental studies of differential cross sections. Such studies have already been performed for three-electron atoms (see, for example, Refs. [8,9,16]). From our previous results on triple ionization [10] and our current on QI we conjecture that the four-electron breakup pattern is also initial state dependent. That is, a regular tetrahedron will be the breakup pattern for initial states where three electrons occupy orbitals with similar spatial distribution. However, while we find that for the ground state of Be the triangular pyramid breakup pattern prevails we also find two more breakup patterns of higher symmetry, namely, a regular tetrahedron and a square previously predicted in Ref. [5]. This suggests the possibility that as the number of electrons increases the prevailing breakup patterns are more consistent with those predicted by Wannier. More theoretical work is needed to explore whether this is indeed the case.

The author A.E. thanks Professor G. Laricchia and Dr. T. Pattard for fruitful discussions and a critical reading of the manuscript. A.E. acknowledges support from the EPSRC under Grant No. EPSRC/H0031771, support from the NSF under Grant No. NSF/0855403, and use of the Legion computational resources at UCL.

[1] G. Zhu, M. Schuricke, J. Steinmann, J. Albrecht, J. Ullrich, I. Ben-Itzhak, T. J. M. Zouros, J. Colgan, M. S. Pindzola, and A. Dorn, Phys. Rev. Lett. **103**, 103008 (2009).

[2] Y. Hikosaka, P. Lablanquie, F. Penent, J. Palaudoux, L. Andric, K. Soejima, E. Shigemasa, I. H. Suzuki, M. Nakano, and K. Ito, Phys. Rev. Lett. **107**, 113005 (2011).

[3] G. H. Wannier, Phys. Rev. **90**, 817 (1953); **100**, 1180 (1955).
[4] H. Klar and W. Schlecht, J. Phys. B **9**, 1699 (1976).
[5] M. Yu. Kuchiev and V. N. Ostrovsky, Phys. Rev. A **58**, 321 (1998).
[6] P. Grujić, Phys. Lett. A **96**, 233 (1983).
[7] A. Emmanouilidou and J. M. Rost, J. Phys. B **39**, 4037 (2006).
[8] J. Colgan, A. Emmanouilidou, and M. S. Pindzola, Phys. Rev. Lett. **110**, 063001 (2013).
[9] X. Ren, A. Dorn, and J. Ullrich, Phys. Rev. Lett. **101**, 093201 (2008).
[10] A. Emmanouilidou, P. Wang, and J. M. Rost, Phys. Rev. Lett. **100**, 063002 (2008).
[11] K. Klunder, J. M. Dahlstrom, M. Gisselbrecht, T. Fordell, M. Swoboda, D. Guenot, P. Johnsson, J. Caillat, J. Mauritsson, A. Maquet, R. Taieb, and A. L'Huillier, Phys. Rev. Lett. **106**, 143002 (2011).
[12] L. R. Moore, M. A. Lysaght, J. S. Parker, H. W. van der Hart, and K. T. Taylor, Phys. Rev. A **84**, 061404(R) (2011); A. S. Kheifets and I. A. Ivanov, Phys. Rev. Lett. **105**, 233002 (2010).
[13] M. Uiberacker, Th. Uphues, M. Schultze, A. J. Verhoef, V. Yakovlev, M. F. Kling, J. Rauschenberger, N. M. Kabachnik, H. Schröder, M. Lezius, K. L. Kompa, H.-G. Muller, M. J. J. Vrakking, S. Hendel, U. Kleineberg, U. Heinzmann, M. Drescher, and F. Krausz, Nature (London) **446**, 627 (2007).
[14] P. Eckle, A. N. Pfeiffer, C. Cirelli, A. Staudte, R. Dörner, H. G. Muller, M. Büttiker, and U. Keller, Science **322**, 1525 (2008).
[15] M. Schultze *et al.*, Science **328**, 1658 (2010).
[16] State-of-the-art quantum mechanical calculations are challenging close to threshold even for three-electrons: J. Colgan, M. S. Pindzola, and F. Robicheaux, Phys. Rev. Lett. **93**, 053201 (2004); J. Colgan and M. S. Pindzola, *ibid.* **108**, 053001 (2012).
[17] T. Schneider, P. L. Chocian, and J. M. Rost, Phys. Rev. Lett. **89**, 073002 (2002).
[18] R. Wehlitz, M. T. Huang, B. D. DePaola, J. C. Levin, I. A. Sellin, T. Nagata, J. W. Cooper, and Y. Azuma, Phys. Rev. Lett. **81**, 1813 (1998).
[19] A. Emmanouilidou and J. M. Rost, J. Phys. B **39**, L99 (2006).
[20] A. Emmanouilidou, Phys. Rev. A **75**, 042702 (2007).
[21] J. Colgan and M. S. Pindzola, J. Phys. B **39**, 1879 (2006).
[22] A. Emmanouilidou, Phys. Rev. A **76**, 054701 (2007).
[23] R. Abrines and I. C. Percival, Proc. Phys. Soc., London **88**, 861 (1966).
[24] D. J. W. Hardie and R. E. Olson, J. Phys. B **16**, 1983 (1983).
[25] E. Wigner, Phys. Rev. **40**, 749 (1932).
[26] N. E. Henriksen, Adv. Chem. Phys. **91**, 433 (1995).
[27] A. Emmanouilidou and J. M. Rost, Phys. Rev. A **75**, 022712 (2007).
[28] A. Emmanouilidou, A. Staudte, and P. B. Corkum, New J. Phys. **12**, 103024 (2010).
[29] G. Sansone, T. Pfeifer, K. Simeonidis, and A. I. Kuleff, ChemPhysChem. **13**, 661 (2012).
[30] H. Price and A. Emmanouilidou (unpublished).